Gold Bull (2011) 44:217–222
DOI 10.1007/s13404-011-0033-6

ORIGINAL PAPER

Gold nanoparticles stabilized by a flake-like Al_2O_3 support

An-Fei An · An-Hui Lu · Qiang Sun · Jie Wang · Wen-Cui Li

Published online: 15 November 2011

Abstract A flake-like alumina with rough surface and small mesopores has been prepared by a hydrothermal method. Remarkably, such alumina was able to stabilize Au nanoparticles, predominantly ~2.2 nm in size, even up to an annealing temperature of 700°C. The catalytic activity was tested using the CO oxidation model reaction where a complete conversion of 1% CO in air at 30°C was obtained.

Keywords Thermostability · Alumina · Gold catalyst · CO oxidation

Introduction

Supported gold catalyst with the gold nanoparticles predominantly below 5 nm in size was discovered to be active for many reactions [1–4]. These catalysts however commonly suffer from high temperature sintering, due to the low Tammann temperature (395°C) of gold, resulting in a significant loss of catalytic activity [5]. Thus, their application is limited where high reaction temperatures are required to prevent catalyst sintering, one feasible solution is to use mesoporous materials [6–9] and hollow cages [10, 11] to provide confined microenvironments for supporting the catalyst. Another is to prepare composite supports by intergrating the advantages of different materials, thus improving the thermal stability and activity of the gold catalyst [12–16]. Examples are CeO_2-doped mesoporous Al_2O_3 [12] and FeO_x-modified hydroxyapatite [16].

A.-F. An · A.-H. Lu · Q. Sun · J. Wang · W.-C. Li (✉)
Dalian University of Technology,
116024 Dalian, China
e-mail: wencuili@dlut.edu.cn

Alumina is a commonly used industrial catalyst support [17]. We describe here a new finding that hydrothermally synthesized Al_2O_3 support using urea as the precipitation agent can retain gold nanoparticles (~2.2 nm) with a high dispersion even after annealing at a temperture of 700°C. The CO oxidation model reaction was used to demonstrate the activity of the annealed Au/Al_2O_3 catalyst.

Experimental

Preparation of Au/Al_2O_3 catalyst

$Al(NO_3)_3{\cdot}9H_2O$ was dissolved in deionized water. Urea was added to the solution as precipitating agent and stirred for 10 min. The molar ratio of $Al(NO_3)_3$: urea was 1:9, and the molar concentration of Al^{3+} was 0.02 M. The obtained solution was decanted into a stainless steel autoclave with a teflon liner and heated at 100°C for 24 h, followed by cooling to room temperature. A white precipitate was filtered and dried at 80°C for 12 h and then denoted as *A1-hydro*. Calcination of *A1-hydro* in air at 500°C for 2 h with a heating rate of 1°C min^{-1}, generated product, named as *A1-500*. For comparison, a conventional Al_2O_3 precursor was prepared by a common precipitation method using 0.02 M $Al(NO_3)_3{\cdot}9H_2O$ aqueous solution as precursor and 0.5 M $(NH_4)_2CO_3$ solution as precipitant under a pH of 8–9. After drying, this precipitant was named as *A2-precip*. Its calcined counterpart was denoted as *A2-500*.

Au/Al_2O_3 catalysts were prepared by a deposition–precipitation (DP) method using a $HAuCl_4$ solution at pH 8–9 (adjusted by 0.5 M $(NH_4)_2CO_3$ solution) in 80°C for 4 h. The samples were washed three times with deionized water, then once with alcohol followed by centrifugal separation and drying in a vacuum. Finally, the samples

were annealed under a flow of air at 250°C or 700°C for 2 h to obtain Au/Al_2O_3 catalysts.

Catalytic test

The catalytic activity of Au/Al_2O_3 in CO oxidation was tested in a fixed bed quartz reactor using 50 mg of catalyst. The total flow rate of the reaction gas was 67 mL min^{-1} with a composition of 1 vol.% CO, 20 vol.% O_2, and 79 vol.% N_2, corresponding to a space velocity of 80,000 mL h^{-1} g_{cat}^{-1}. The products were analyzed using a GC-7890 gas chromatograph equipped with a thermal conductivity detector.

Catalytic characterization

Thermogravimetric and differential scanning calorimetry analyses (TG-DSC) were conducted on a thermogravimetric analyzer STA 449 F3 Jupiter (NETZSCH) under an air atmosphere with a heating rate of 10°C min^{-1}. Transmission electron microscope (TEM) images were obtained with a Tecnai G220 S-Twin microscope with accelerative voltage of 200 kV. Scanning electron microscope (SEM) images were obtained with a Hitachi S-4800 instrument. X-ray diffraction (XRD) was performed with a D/MAX-2400 diffractometer using Cu K_α radiation. Nitrogen sorption isotherms were measured with a Micromeritics TriStar 3000 adsorption analyzer. The gold content was analyzed using an inductively coupled plasma atomic emission spectrometer (ICP-AES) on the Optima 2000 DV.

Results and discussion

Sample properties

First of all, TG-DSC measurement was employed to analyze the thermal behavior of the uncalcined alumina precursors *A1-hydro* and *A2-precip* and the corresponding curves are complied in Fig. 1a, b. As expected, *A1-hydro* shows a different thermal decomposition behavior from *A2-precip*. The weight loss (~18%) of *A1-hydro* continues until 450°C which corresponds to the displacement of physically adsorbed water below 100°C, dehydration of aluminum hydroxide and finally transition to γ-alumina. When the temperature exceeds 450°C, no obvious weight loss is observed indicating aluminum hydroxide has transferred to aluminum oxide. Under the same thermal treatment conditions, *A2-precip* shows a remarkable weight loss (~38%) up to 450°C. Calcination of aluminum hydroxide usually involves the following two reactions [18]:

$$2AlO(OH) \rightarrow Al_2O_3 + H_2O \quad (1)$$

$$2Al(OH)_3 \rightarrow Al_2O_3 + 3H_2O \quad (2)$$

If boehmite or pseudo-boehmite is the primary precipitate, reaction (1) should dominate with a ~15% weight loss accompanied with calcination. If reaction (2) is the primary one, ~34.6% weight loss should be observed after calcination. Based on the above results, we can infer that the as-prepared alumina precursor *A1-hydro* is mainly composed of AlO(OH) and *A2-precip* is $Al(OH)_3$.

The DSC curves of *A1-hydro* and *A2-precip* (Fig. 1b) display an exothermic peak up to 900°C. However, the height of the exothermic peak of *A1-hydro* is lower than that of *A2-precip*, indicating a lower thermal shrinkage and easier phase transition of *A1-hydro*. Furthermore, *A1-hydro* and *A2-precip* were calcined at 500°C in air and then characterized with XRD.

As seen in Fig. 2a, although calcined samples *A1-500* and *A2-500* can both be assigned to a γ-Al_2O_3 phase (JCPDS card no. 10-0425), the diffraction peaks of *A2-500* are rather weak, indicating a proportion of amorphous phase in the skeleton. The XRD patterns of the gold supported alumina catalysts do not show clear diffraction peaks of the gold nanoparticles, that strongly indicates the deposited gold particles are small in sizes. This is consistent with the TEM observation in Fig. 4. The porosity of the alumina was

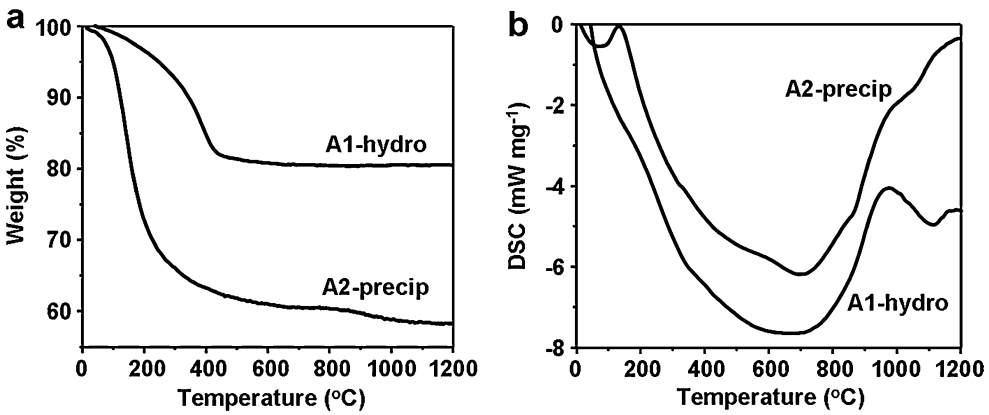

Fig. 1 **a** TG and **b** DSC curves of the as-synthesized alumina precursors *A1-hydro* and *A2-precip*

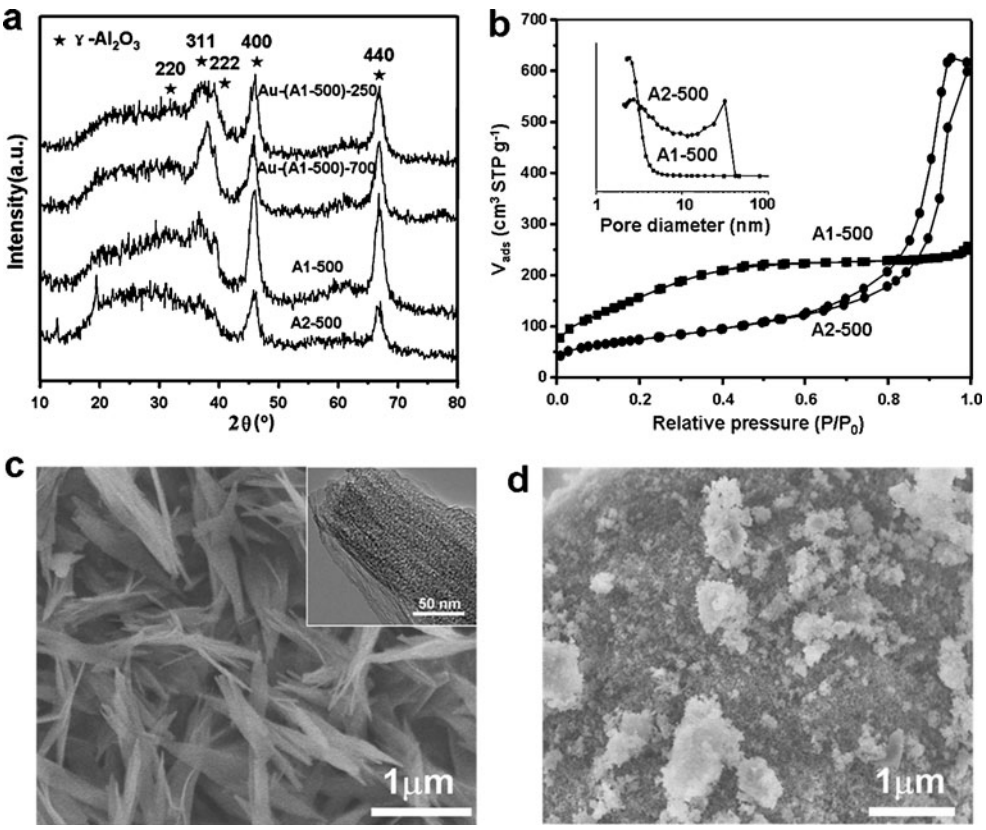

Fig. 2 **a** XRD patterns, **b** nitrogen sorption isotherms, inset with pore size distributions deduced from the desorption branches; SEM images of alumina *A1-500* (**c**, inset is the TEM image) and *A2-500* (**d**)

characterized using nitrogen sorption at 77 K. As seen in Fig. 2b, the nitrogen sorption isotherms of *A1-500* and *A2-500* are essentially of type IV. The isotherm of *A1-500* has a small continuous nitrogen uptake at P/P_0=0.2–0.5, indicating the presence of small mesopores; while the isotherm of *A2-500* has a sharp capillary condensation step at P/P_0=0.8–1.0, indicative of the presence of larger mesopores, possibly constructed from the closely packed the flake-like alumina. The pore size distributions, determined from the desorption branches of the isotherms by the Barrett–Joyner–Halenda method, show that *A1-500* has a narrow mesopore size distribution centered at 2.5 nm, whereas *A2-500* shows a rather broad distribution with mesopore sizes concentrated at 3.0 and 35 nm. *A2-500* exhibits a higher BET surface area (268 $m^2\ g^{-1}$) and total pore volume (0.93 $m^3\ g^{-1}$) than that of *A1-500* (222 $m^2\ g^{-1}$ and 0.34 $m^3\ g^{-1}$, accordingly). Furthermore, the morphologies of these two samples were characterized by SEM. Hydrothermally synthesized *A1-500* shows distinct flake-like features (Fig. 2c); while *A2-500* prepared using a precipitation method has an undefined morphology (Fig. 2d).

Catalytic activity

Alumina *A1-500* and *A2-500* were used as supports to load gold nanoparticles by a DP method. The obtained catalysts were named as *Au*-(*A1-500*) and *Au*-(*A2-500*). The actual gold contents by weight were 2.08 wt.% for *Au*-(*A1-500*) and 1.89 wt.% for *Au*-(*A2-500*), as determined by an ICP-AES technique. Prior to a catalytic test, the catalysts were annealed in air at 250°C and 700°C, respectively, and the corresponding catalysts were denoted *Au*-(*A1-500*)-*250*, *Au*-(*A2-500*)-*250*, *Au*-(*A1-500*)-*700* and *Au*-(*A2-500*)-*700*. As shown in Fig. 3, catalyst *Au*-(*A1-500*)-*250* shows a high activity and 1% CO can be completely oxidized to CO_2 at 10°C, which is a significantly higher activity as compared to most reported Au/Al_2O_3 catalysts [12, 19]. The TEM image (Fig. 4a) shows that gold nanoparticles in sample *Au*-

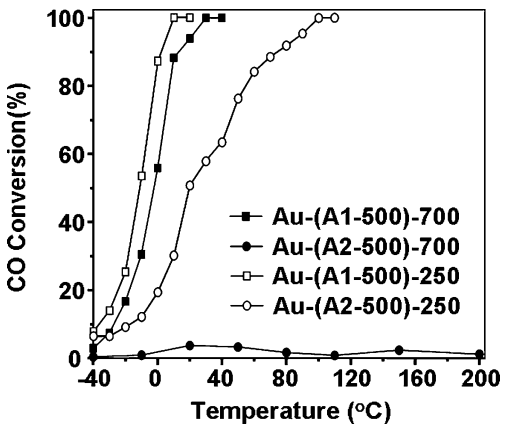

Fig. 3 CO conversion of the gold nanoparticles supported on different alumina supports and calcined at different temperatures

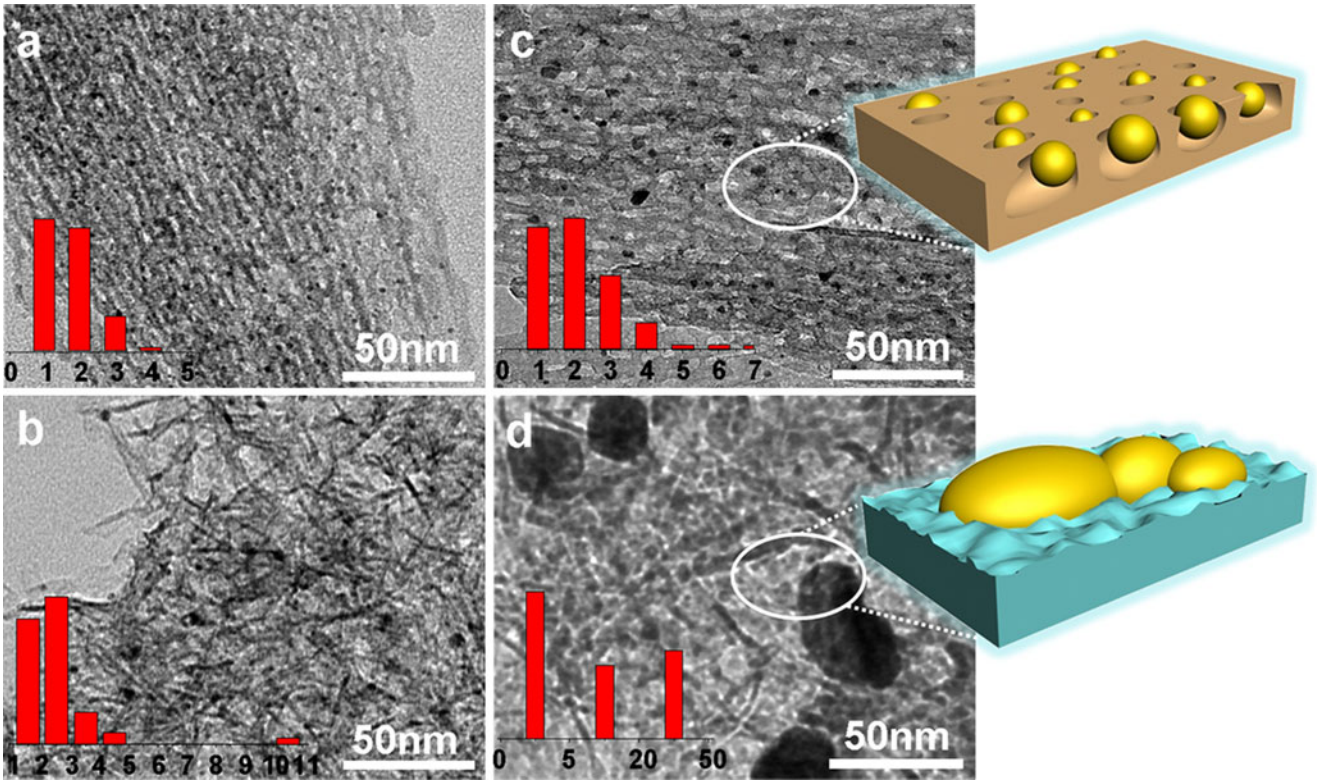

Fig. 4 TEM images of Au/Al_2O_3 catalysts (**a** *Au-(A1-500)-250*, **b** *Au-(A2-500)-250*, **c** *Au-(A1-500)-700*, **d** *Au-(A2-500)-700*)

(*A1-500*)-*250* are highly dispersed and an average particle size of ~1.8 nm is determined from TEM images by measuring a minimum of 200 gold particles. The small gold particle size and high activity of the catalyst for CO oxidation confirmed the finding of Häkkinen's work [4]. In the case of *Au-(A2-500)-250* catalyst, the temperature of complete CO conversion ($T_{100\%}$) rises sharply up to 100°C (see Fig. 3). In addition, based on the results from Fig. 3, the estimated reaction rates (listed in Table 1) indicate that the flake-like alumina is an active catalyst support. As shown by the TEM image in Fig. 4b, many gold particles of ~ 3 nm size are present, which are larger than those (~1.8 nm) of *Au-(A1-500)-250*. In addition, some even larger gold nanoparticles with sizes ~10 nm are also observed. It is common that gold tends to form large particles (>7 nm) on a conventional Al_2O_3 support when the catalyst is prepared by the DP method [20].

To date, in the absence of an additional promoter (e.g., CeO_2) for the support, active Au/Al_2O_3 catalyst with high-temperature resisting was hardly found. This is due to the low Tammann temperature of gold nanoparticles which generally tend to melt and sinter at high temperature. Surprisingly, in our case, the catalyst *Au-(A1-500)-700* calcined at 700°C shows a high activity and the complete conversion of CO can be achieved at a temperature as low as 30°C (Fig. 3). In contrast, the catalyst *Au-(A2-500)-700*, synthesized using the common precipitation method shows no activity (Fig. 3). This experiment was repeated three times and identical results confirmed the reproducibility. According to the literature and our present results, we preliminarily attributed the flake-like alumina support play an important role in stabilizing the gold nanoparticles during high-temperature annealing. To understand that, we therefore further characterized this catalyst using TEM. As seen in Fig. 4c, the TEM image shows that the diameter of the gold nanoparticles in sample *Au-(A1-500)-700* is *ca.* 2.2 nm in size. This reveals that the gold nanoparticles must be trapped/stabilized by the alumina support, which can be related to its unique flake-like morphology. By carefully comparing the TEM images in Fig. 4, it can be seen that the surfaces of thin flakes on the *A1-500* support are very rough

Table 1 Estimated reaction rates

Sample	Au (at.%)	T(K)	Rate (mol h^{-1} g_{Au}^{-1})	TOF(s^{-1})[a,b]
Au-(A1-500)-700	2.08	293	1.508	0.0825
Au-(A2-500)-700	1.89	293	0.053	0.0029
Au-(A1-500)-250	2.08	293	1.604	0.0878
Au-(A2-500)-250	1.89	293	0.884	0.0484

[a] Turnover frequency was calculated based on the number of the supported Au atoms

[b] The value of TOF in literature[24, 25] is <0.009 s^{-1}

and contain numerous small and surface orientated mesopores. The presence of small mesopores has been confirmed by the aforementioned nitrogen sorption measurement. These shallow small mesopores should act as containers which prevent the gold nanoparticles from escaping and sintering, and thus enabling an excellent activity and thermostability. In contrast, the TEM image of *Au-(A2-500)-700* (Fig. 4d) shows significant sintering of gold nanoparticles with sizes greater than 20 nm after thermal annealing at 700°C. Theoretically, to form one spherical particle with a diameter of 20 nm would require the merging of 1,000 particles with a diameter of 2 nm. It is clear that the sintering of gold particles is responsible for the complete loss of CO oxidation activity [5]. Hence, we proposed that the unique structure of such thin flake alumina *A1-500* with numerous small mesopores may provide structural defects and cavity (see the scheme illustration in Fig. 4), which hinder the mobility and sintering of the supported gold nanoparticles [21, 22]. This in principle is similar to the previous finding that Pt nanoparticles can be stabilized on carbon supports with rough surface and cavities [23].

Conclusions

It has been discovered that hydrothermally synthesized flake-like alumina is able to stabilize gold nanoparticles with small sizes (predominantly ~2.2 nm) and high dispersion, even after annealing of the catalyst to 700°C. The high activity of such a catalyst was proven using the model CO oxidation reaction as evidenced by a complete conversion of CO at 30°C. The very rough surface and numerous small mesopores on this alumina support were found to be responsible for the stabilization of the gold nanoparticles. Such an alumina could be an ideal candidate for the preparation of high temperature stable catalysts, e.g., catalyst for the water gas shift reaction.

Acknowledgments The project was supported by the National Natural Science Foundation of China (no. 20973031) and New Century Excellent Talents in University of China (NCET-08-0075).

References

1. Haruta M (2002) Catalysis of gold nanoparticles deposited on metal oxides. CATECH 6:102–115
2. Bond GC, Thompson DT (2000) Gold-catalysed oxidation of carbon monoxide. Gold Bull 33:41–51
3. Hashmi ASK, Hutchings GJ (2006) Gold catalysis. Angew Chem Int Ed 45:7896–7936
4. Lopez-Acevedo O, Kacprzak KA, Akola J, Hakkinen H (2010) Quantum size effects in ambient CO oxidation catalysed by ligand-protected gold clusters. Nat Chem 2:329–334
5. Wen L, Fu JK, Gu PY, Yao BX, Lin ZH, Zhou JZ (2008) Monodispersed gold nanoparticles supported on γ-Al_2O_3 for enhancement of low-temperature catalytic oxidation of CO. Appl Catal B 79:402–409
6. Sun JM, Ma D, Zhang H, Liu XM, Han XW, Bao XH, Weinberg G, Pfänder N, Su DS (2006) Toward monodispersed silver nanoparticles with unusual thermal stability. J Am Chem Soc 128:15756–15764
7. Chiang CW, Wang AQ, Mou CY (2006) CO oxidation catalyzed by gold nanoparticles confined in mesoporous aluminosilicate Al-SBA-15: pretreatment methods. Catal Today 117:220–227
8. Bandyopadhyay M, Korsak O, van den Berg MWE, Grünert W, Birkner A, Li WC, Schüth F, Gies H (2006) Gold nano-particles stabilized in mesoporous MCM-48 as active CO-oxidation catalyst. Micropor Mesopor Mat 89:158–163
9. Gabaldon JP, Bore M, Datye AK (2007) Mesoporous silica supports for improved thermal stability in supported Au catalysts. Top Catal 44:253–262
10. Arnal PM, Comotti M, Schüth F (2006) High-temperature-stable catalysts by hollow sphere encapsulation. Angew Chem Int Ed 45:8224–8227
11. Joo SH, Park JY, Tsung CK, Yamada Y, Yang PD, Somorjai GA (2009) Thermally stable Pt/mesoporous silica core–shell nanocatalysts for high-temperature reactions. Nat Mater 8:126–131
12. Yuan Q, Duan HH, Li LL, Li ZX, Duan WT, Zhang LS, Song WG, Yan CH (2010) Homogeneously dispersed Ceria nanocatalyst stabilized with ordered mesoporous alumina. Adv Mater 22:1475–1478
13. Yan W, Mahurin SM, Pan Z, Overbury SH, Dai S (2005) Ultrastable Au nanocatalyst supported on surface-modified TiO_2 nanocrystals. J Am Chem Soc 127:10480–10481
14. Min BK, Wallace WT, Goodman DW (2004) Synthesis of a sinter-resistant, mixed-oxide support for Au nanoclusters. J Phys Chem B 108:14609–14615
15. Zhu HG, Ma Z, Overbury SH, Dai S (2007) Rational design of gold catalysts with enhanced thermal stability: post modification of Au/TiO_2 by amorphous SiO_2 decoration. Catal Lett 116:128–135
16. Zhao KF, Qiao BT, Wang JH, Zhang YJ, Zhang T (2011) A highly active and sintering-resistant Au/FeO_x–hydroxyapatite catalyst for CO oxidation. Chem Commun 47:1779–1781
17. Li WC, Comotti M, Lu AH, Schüth F (2006) Nanocast mesoporous $MgAl_2O_4$ spinel monoliths as support for highly active gold CO oxidation catalyst. Chem Commun 16:1772–1774
18. Ram S, Rana S (2000) Synthesis of mesoporous clusters of AlO(OH)·αH_2O by a surface hydrolysis reaction of pure Al-metal with nascent-surface in water. Mater Lett 42:52–60
19. Grisel RJH, Nieuwenhuys BE (2001) Selective oxidation of CO, over supported Au catalysts. J Catal 199:48–59
20. Chen YJ, Yeh CT (2001) Deposition of highly dispersed gold on alumina support. J Catal 200:59–68
21. Wallace WT, Min BK, Goodman DW (2005) The stabilization of supported gold clusters by surface defects. J Mol Catal A 228:3–10
22. Veith DM, Lupini AR, Rashkeev S, Pennycook SJ, Mullins DR, Schwartz V, Bridges CA, Dudney NJ (2009) Thermal stability and

catalytic activity of gold nanoparticles supported on silica. J Catal 262:92–101
23. Reetz MT, Schulenburg H, Lopez M, Spliethoff B, Tesche B (2004) Platinum-nanoparticles on different types of carbon supports: Correlation of electrocatalytic activity with carrier morphology. Chimia 58:896–899
24. Kung HH, Kung MC, Costello CK (2003) Supported Au catalysts for low temperature CO oxidation. J Catal 216:425–432
25. Lee S-J, Gavriilidis A (2002) Supported Au catalysts for low-temperature CO oxidation prepared by impregnation. J Catal 206:305–313